Dexterous Workspace of n-RRRR and n-RRPR Manipulators

André Gallant[1], Roger Boudreau[2], Marise Gallant[3]

[1] *Département de Génie Mécanique, Université de Moncton, eag3440@umoncton.ca*

[2] *Département de Génie Mécanique, Université de Moncton, roger.a.boudreau@umoncton.ca*

[3] *Département de Génie Mécanique, Université de Moncton, marise.gallant@umoncton.ca*

Abstract

In this work, a geometric method is presented to determine the dexterous workspace of two architectures of kinematically redundant planar parallel manipulators. The architectures studied are n-RRRR and n-RRPR[4] . These architectures are characterized by having a revolute actuator as the kinematically redundant actuator added to the base of each kinematic chain. First, the dexterous workspace of the non-redundant part (RRR or RPR) of each kinematic chain is studied. Then the effect of the redundant actuator is considered to yield a geometric representation of the dexterous workspace of each kinematic chain. The intersection of the dexterous workspaces of all kinematic chains of a manipulator is determined to obtain the geometric representation of the dexterous workspace. Finally, the Gauss Divergence Theorem is applied to compute the area of the dexterous workspace. An example is given to demonstrate an application of the method.

Keywords: kinematic redundancy, planar parallel manipulator, dexterous workspace, RRRR, RRPR

Espace dextre des manipulateurs n-RRRR et n-RRPR

Résumé

Ce travail consiste à déterminer l'espace dextre des manipulateurs n-RRRR et n-RRPR en utilisant une méthode géométrique. Premièrement, l'espace dextre des parties non-redondantes (RRR ou RPR) est déterminé. Ensuite, l'effet de l'articulation redondante est considéré pour donner une représentation géométrique de l'espace dextre de chaque chaîne cinématique. L'intersection des espaces dextres de chaque chaîne est alors déterminée pour obtenir la représentation géométrique de l'espace dextre du manipulateur. Enfin, le théorème de divergence de Gauss est appliqué pour calculer la surface de l'espace dextre. Un exemple est illustré afin de démontrer la méthode.

Mots-clé: redondance cinématique, manipulateur parallèle plan, espace dextre, RRRR, RRPR

[4]The parallel manipulators considered consist of n serial kinematic chains that connect the end-effector to the base. R indicates a revolute joint and P indicates a prismatic joint. Underlined letters in the notation indicate that the joint is actuated.

1 INTRODUCTION

The shape and size of the dexterous workspace can be used to evaluate and to compare the dimensions of a given architecture or to compare different architectures. The dexterous workspace for planar manipulators can be defined as the area where the end-effector is able to reach with any orientation.

Several researchers have studied the dexterous as well as other types of workspace for the non-redundant 3-RRR symmetric planar architecture [1, 2, 3]. The dexterous workspace in these works was defined by a maximum of two concentric circles for each of the three kinematic chains. For the 3-RRR architecture, a dexterous workspace of two concentric circles per chain can be called the controllably dexterous workspace where the dexterous workspace is devoid of discontinuities [3]. Zhaohui and Zhonghe [4] identified a third concentric circle near the base of each kinematic chain by using the four-bar mechanism analogy on a symmetric 3-RRR manipulator. Work has also been done to determine various workspaces of planar parallel manipulators including the 3-RRR and the 3-RPR manipulators [5].

Several works have used an integration of the workspace boundary based on the Gauss Divergence Theorem [6] to obtain its surface area [1, 7].

Ebrahimi et al. [8] introduced new kinematically redundant manipulators by adding a prismatic actuator to the base of each kinematic chain of the 3-RRR manipulator architecture. The dexterous workspace of these kinematically redundant manipulators was obtained with a discreet method which is computationally inefficient and does not yield an exact solution.

A method similar to the one presented in this work was applied to the n-PRRR manipulator [9, 10]. The determination of the dexterous workspace of planar n-RRRR and n-RRPR manipulators, or of hybrid n-RRRR-m-RRPR manipulators, is the object of this work. In what follows, in order to alleviate the text, the term workspace will denote the dexterous workspace.

The next section of this work presents the architectures studied. The method is then explained in section 3 beginning with the dexterous workspace of the non-redundant parts of the kinematic chains followed by the determination of the dexterous workspace of the redundant chains. Then the workspace of the redundant manipulators is studied and examples are given to illustrate the application of the method. Finally, a conclusion is presented.

2 ARCHITECTURES

In Fig. 1, examples of the architectures studied are illustrated. Figure 1(a) shows an example 3-RRRR manipulator whereas Fig. 1(b) shows an example 3-RRPR manipulator. It can be seen that the n-RRRR and the n-RRPR manipulators are based on the well known 3-RRR and 3-RPR manipulators, respectively. In both of these manipulator architectures, the redundant actuator is a revolute actuator and a link is added to the base of each kinematic chain. As a result, the dexterous workspaces of these manipulators are very similar.

3 METHODOLOGY

The basic concepts of the method described in this work can be applied to many different planar parallel architectures. The method can be summarized by the following five steps:

1. Determine the boundaries of the workspace of each kinematic chain.
2. Determine all points of intersection between the boundaries of the workspace of each kinematic chain.

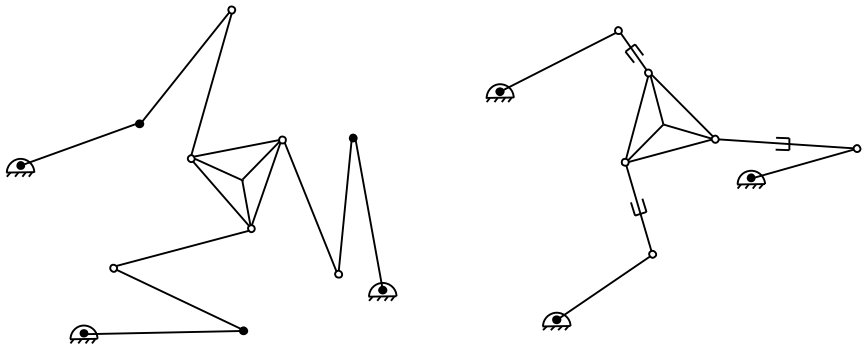

(a) 3-RRRR (b) 3-RRPR

Figure 1: Example 3-RRRR and 3-RRPR planar parallel manipulators.

3. Segment the boundaries of the workspace of each kinematic chain at each of their points of intersection.
4. Determine which of these segments form the boundaries of the workspace of the manipulator.
5. Compute the contribution of each segment in the workspace and add them to obtain the area of the workspace of the manipulator.

3.1 Workspace of RRR Kinematic Chains [10]

Step 1 in the method to determine the workspace of these manipulator architectures is determining the boundaries of the workspace of each kinematic chain. In order to obtain this, the non-redundant part of each kinematic chain architecture must first be considered. The effect of the redundant actuator can then be considered to determine the boundaries of each redundant kinematic chain.

The first architecture to be studied is the RRR non-redundant portion of the RRRR kinematic chain. Figure 2 shows an example RRR kinematic chain, where (X_1, Y_1) are the coordinates of the base of the kinematic chain and (X_2, Y_2) are the coordinates of the end-effector. The length of the proximal link is denoted by L_1, L_2 is the length of the distal link, and L_3 is the length of the link that connects the distal link to the end-effector (represents the platform). Finally, L_0 is the distance separating (X_1, Y_1) and (X_2, Y_2) for a given posture. It can be seen that (X_1, Y_1), L_1, L_2, and L_3 are constant, whereas (X_2, Y_2) and L_0 vary with the position of the end-effector.

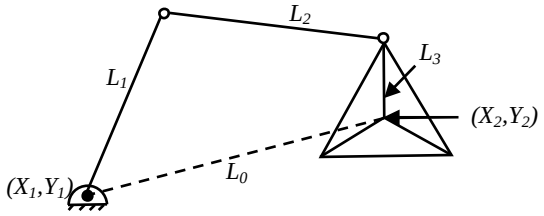

Figure 2: Example RRR kinematic chain.

With the relationships between the constant link lengths L_1, L_2 and L_3, three classes of workspace for RRR kinematic chains can be identified using a four-bar mechanism analogy. These classes are shown in Fig. 3 where it can be seen that the workspace of RRR kinematic chains is defined

by one, two or three concentric circles defining a workspace of Class 1, 2 or 3, respectively. The radius of each concentric circle, defined by r_1, r_2 or r_3, are defined by the following [10]:

$$\begin{aligned} r_1 &= S + M - L \\ r_2 &= |L_1 - L_2| + L_3 \\ r_3 &= L_1 + L_2 - L_3 \end{aligned} \tag{1}$$

where S is the length of the shortest link, L is the length of the longest link and M is the length of the other link.

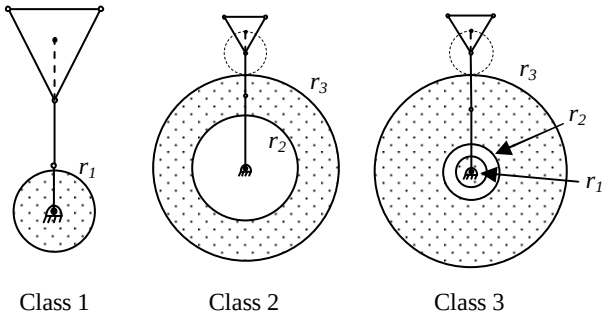

Figure 3: Workspace classes for RRR kinematic chains.

The concept behind the method used to determine these classes is that for a given end-effector position, if the link of length L_3 is a crank, in the four-bar mechanism analogy, that position is part of the workspace of the non-redundant kinematic chain. When the position of the end-effector changes, the length L_0 changes and at specific lengths, the resulting four-bar mechanism changes category. When the category of the mechanism is double crank and crank rocker, with L_3 as the crank, the end-effector is in the workspace. Thus, finding the lengths L_0 that permit L_3 to be a crank forms circles that define the workspace of the non-redundant kinematic chain. Table 1 shows the conditions under which each concentric circle defines a boundary of the workspace of the RRR kinematic chain.

Table 1: Conditions for each RRR kinematic chain class.

	No link longer than sum of others	**One link longer than sum of others**
$\boldsymbol{L_3}$ **shortest**	Class 3 (r_1, r_2 and r_3)	Class 2 (r_2 and r_3)
$\boldsymbol{L_3}$ **not shortest**	Class 1 (r_1)	No workspace

3.2 Workspace of RPR Kinematic Chains

Similarly to the n-RRRR manipulator architecture, the n-RRPR architecture is based on the 3-RPR manipulator with a revolute redundant actuator at the base of each kinematic chain. Again, the non-redundant portion of the kinematic chain can be studied separately from the effect of the redundant actuator. An example RPR kinematic chain is shown in Fig. 4 where L_1 is the length of the prismatic actuator for a given posture, L_1^{min} and L_1^{max} are the minimum and maximum lengths of the prismatic actuator, respectively. The length of the link representing the platform of the end-effector is denoted by L_3, (X_1, Y_1) are the coordinates of the base of the RPR kinematic chain, and (X_2, Y_2) are the coordinates of the end-effector for a given posture.

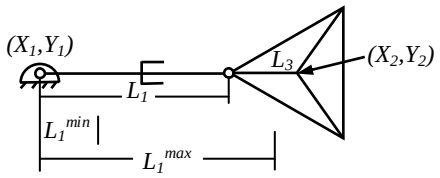

Figure 4: Example RPR kinematic chain.

The workspace of kinematic chains of this architecture belongs to one of the same three classes as the RRR kinematic chains. The range of motion of the prismatic joint must be sufficient for the platform to be able to complete a full rotation for any point inside the workspace. Figure 5 illustrates the extreme positions for kinematic chains of Class 1 and Class 2. From this Fig., the radius of each concentric circle that forms the workspace of RPR chains can be determined by the following equation:

$$\begin{aligned} r_1 &= min\{L_3 - L_1^{min}, L_1^{max} - L_3\} \\ r_2 &= L_1^{min} + L_3 \\ r_3 &= L_1^{max} - L_3 \end{aligned} \tag{2}$$

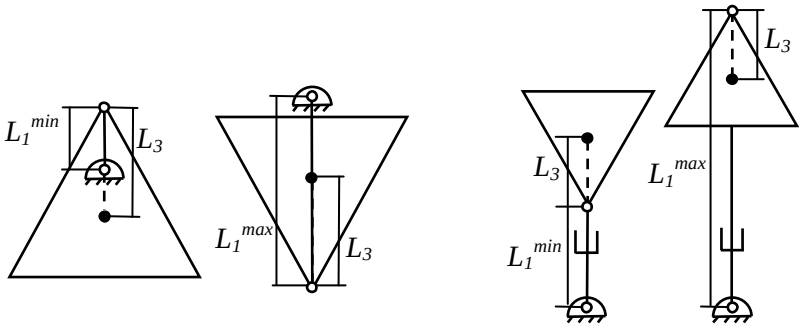

(a) Class 1 ($L_1^{min} < L_3$) (b) Class 2 ($L_1^{max} - L_1^{min} > 2L_3$)

Figure 5: Extreme positions of RPR kinematic chains.

Depending on whether or not the RPR chain respects the following two inequalities, the workspace is defined by different classes.

$$L_1^{min} < L_3 \quad \text{(Inequality A)} \tag{3}$$

$$L_1^{max} - L_1^{min} > 2L_3 \quad \text{(Inequality B)} \tag{4}$$

In Eq. (2), when Inequality A is false, radius r_1 becomes negative and there is no workspace of Class 1. For a Class 2 workspace to exist, radius r_3 must be larger than r_2, producing Inequality B. When both inequalities are true, both workspaces exist, producing a Class 3 workspace.

Table 2 summarizes the classes of workspace obtained for every combination of these inequalities.

Table 2: Resulting classes in each combination of inequalities A and B.

Inequality		**Resulting workspace**
A	**B**	**Class**
True	False	1
False	True	2
True	True	3
False	False	No dexterous workspace

3.3 Workspaces of Redundant RRRR and RRPR Kinematic Chains

As seen in the two previous sub-sections, the workspace of the non-redundant portions of RRRR and RRPR kinematic chains are defined by the same three classes. Therefore, the effect of the redundant actuator on the final workspace of these two chain architectures is the same. It follows that the workspace of manipulators with kinematic chains of either of these architectures, or even a combination of both, can be determined in the same way.

The workspaces of redundant RRRR and RRPR kinematic chains are dependent on the class of the non-redundant portion and its associated radii, as well as the length of the redundant link. In Figs. 2 and 4, the point (X_1, Y_1) is considered to be fixed. The workspace of non-redundant RRR and RPR chains is thus centered at this point. However, when the redundant actuator and its link are considered, the center of the workspace is no longer fixed but moves along a set trajectory. This trajectory is simply a circle of radius equal to the length of the redundant link L_4.

Figure 6 shows example RRRR and RRPR kinematic chains. In this Fig., the dimensions of the non-redundant chain are the same as in Figs. 2 and 4, L_4 is the length of the redundant link and (X_3, Y_3) are the coordinates of the base point of the new chain. As stated above, the point (X_1, Y_1) moves along a circle of radius L_4 centered at point (X_3, Y_3).

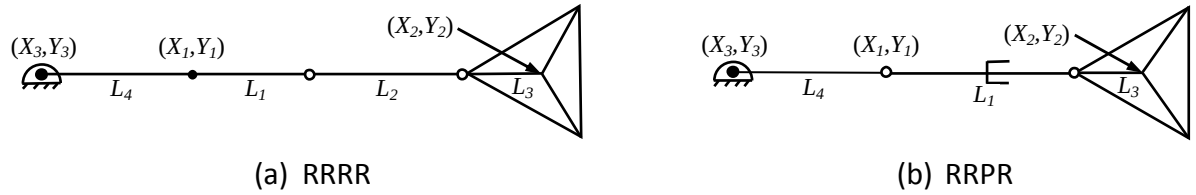

Figure 6: Example RRRR and RRPR kinematic chains.

For each position of the redundant actuator, the resulting workspace has the form of one of the three classes described in the two previous sub-sections. Therefore, when the point (X_1, Y_1) moves, so too does the workspace. Since the redundant actuator can move freely, the workspace of the redundant chain is the union of the workspace of the non-redundant portion at every possible position of the redundant actuator. In other words, the workspaces of the RRRR and RRPR chains are analogous to a marker, the shape of one of the classes discussed above, being dragged along a trajectory defined by a circle of radius L_4 centered at point (X_3, Y_3).

The effect of the redundant actuator is studied considering each of the classes of workspace of the non-redundant portion of the kinematic chain, starting with Class 1. Figure 7 shows the two cases and the two resulting types of workspace possible with chains of workspace of Class 1. In what follows, workspaces are defined as Type X, where X indicates the number of circles needed to define it. In this Fig., it can be seen that when L_4 is shorter than the radius r_1, such as in Fig. 7(a), only one circle defines the workspace of the redundant chain. However, when L_4 is longer than r_1, a second circle forming an inner boundary is observed. Such is the case of the workspace of Type 2 shown in Fig. 7(b). In the Figures of this section, the dashed circle shows the trajectory of the center of the non-redundant workspace. Table 3 summarizes the types of workspace, the associated radii and the conditions for workspaces resulting from Class 1 workspaces.

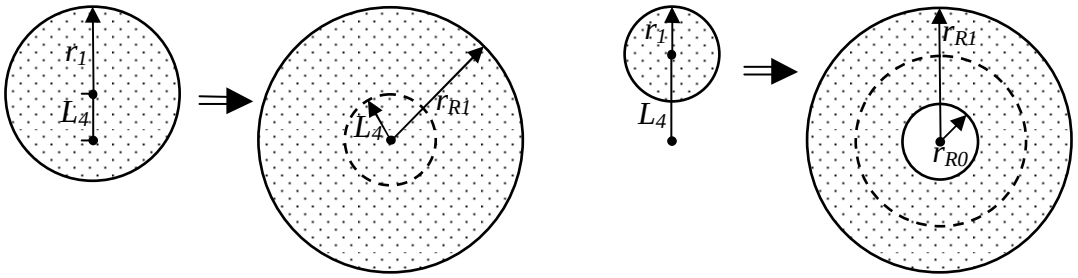

(a) Type 1 (b) Type 2

Figure 7: Workspace types resulting from Class 1 non-redundant workspaces.

Table 3: Conditions and radii of the workspace types resulting from Class 1 workspaces.

Type	**Condition**	**Radii**	**Figure**
1	$L_4 \leq r_1$	$r_{R1} = L_4 + r_1$	7(a)
		$r_{R0} = L_4 - r_1$	
2	$L_4 > r_1$	$r_{R1} = L_4 + r_1$	7(b)

Figure 8 shows the possible workspaces resulting from Class 2 non-redundant workspaces. It can be seen from this Fig. that when L_4 is shorter than r_2, the resulting workspace is of Type 2, as can be seen in Fig. 8(a). When L_4 is longer than r_2 but shorter than r_3, the resulting workspace is of Type 1, as seen in Fig. 8(b). Finally, when L_4 is longer than r_3, the resulting workspace is of Type 2 again, which is similar to the Type 2 workspace seen in Fig. 7(b). Table 4 summarizes the types, the radii and the conditions of workspaces resulting from Class 2 non-redundant workspaces. Note that the definition of r_{R0} in workspaces resulting from Class 1 is slightly different from the one in workspaces resulting from Class 2 (See Tables 3 and 4).

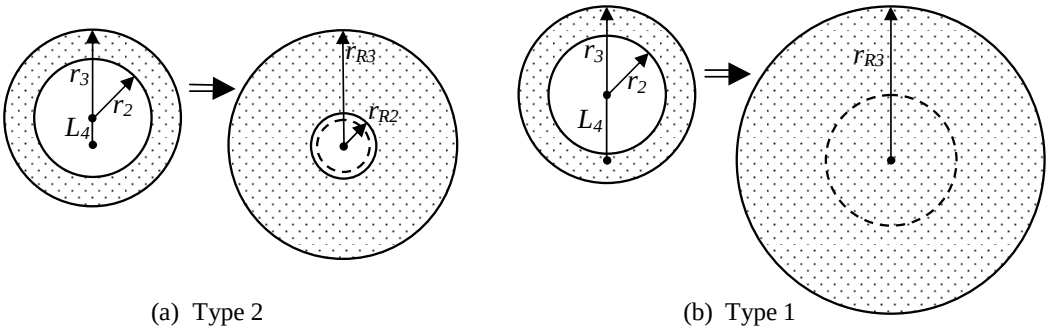

(a) Type 2 (b) Type 1

Figure 8: Workspace types resulting from Class 2 non-redundant workspaces.

Table 4: Conditions and radii of the workspace types resulting from Class 2 workspaces.

Type	**Condition**	**Radii**	**Figure**
		$r_{R2} = r_2 - L_4$	
2	$L_4 < r_2$	$r_{R3} = L_4 + r_3$	8(a)
1	$r_2 \leq L_4 \leq r_3$	$r_{R3} = L_4 + r_3$	8(b)
		$r_{R0} = L_4 - r_3$	
2	$L_4 > r_3$	$r_{R3} = L_4 + r_3$	

The last non-redundant workspace class to be studied is the Class 3. Due to the third circle defining this non-redundant workspace, a greater number of resulting workspace types are identified. When L_4 is sufficiently small, a Type 3 workspace is obtained as shown in Fig. 9.

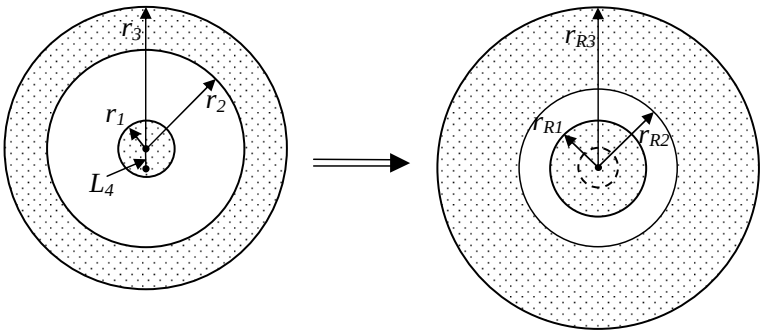

Figure 9: Example workspace of Type 3 resulting from a Class 3 non-redundant workspace.

When L_4 increases, the radius $r_{R1} = r_1 + L_4$ becomes larger while $r_{R2} = r_2 - L_4$ becomes smaller. For the annular non-dexterous workspace to exist, $r_{R1} < r_{R2}$ must be true, or:

$$L_4 < \frac{r_2 - r_1}{2} \tag{5}$$

For the annular region to disappear ($L_4 \geq \frac{r_2 - r_1}{2}$) while L_4 is still inside the region defined by r_1 ($L_4 < r_1$), the following condition is necessary:

$$r_2 \leq 3r_1 \tag{6}$$

When this condition is true, the workspace will henceforth be considered a Category A while when it is false, the workspace will be considered a Category B. Thus, Category A workspaces will not possess a non-dexterous annular workspace defined by r_{R1} and r_{R2} unless L_4 respects Eq. (5). The distinction between the two categories is important since the relationships between L_4 and the radii of the non-redundant workspaces required to define the redundant workspaces are different as will be shown shortly. Figure 10 shows the difference between these two categories of workspace when the redundant actuator is considered.

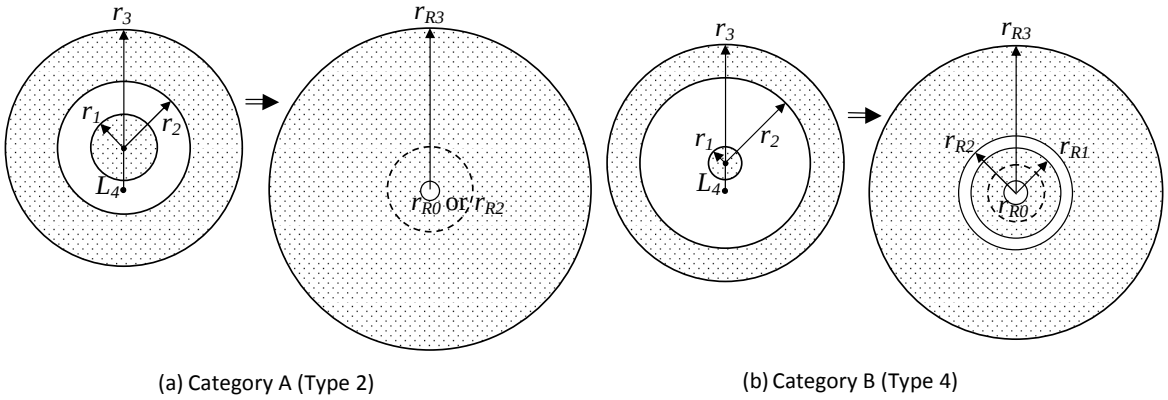

Figure 10: Two categories of Class 3 workspaces.

From this Fig., the differences between the two categories of Class 3 workspaces can be observed when L_4 is slightly longer than r_1. With manipulators of Category A, a workspace of Type 4 is not possible because, when L_4 is slightly longer than r_1, the circle of radius r_{R1} has already made contact with the circle of radius r_{R2}, as seen in Fig. 10(a). On the other hand, with workspaces of category B the circles of radii r_{R1} and r_{R2} do not make contact even when L_4 is slightly longer than r_1. With workspaces of this category, when L_4 is slightly longer than r_1, the resulting workspace is of Type 4 as seen in Fig. 10(b).

Table 5 summarizes the types, the conditions and the radii associated with the workspaces possible from Class 3 non-redundant workspaces of Category A and Table 6 shows the same for Category B workspaces. From these tables, the differences between the two categories of Class 3 workspaces can be readily seen. These tables are ordered in ascending length L_4 to better illustrate the conditions under which each type of workspace is the result of the effect of the redundant actuator. To clarify some of the expressions in the tables, note that when $L_4 > r_1$, the radius of the hole in the inner workspace is the smallest between $L_4 - r_1$ and $r_2 - L_4$ (see Fig. 10(a)). They are equal when $L_4 = \frac{r_1+r_2}{2}$. Due to space limitations, some conditions and their resulting workspace types have no associated figures as can be seen in Tables 5 and 6. However, all four types of RRRR and RRPR workspace are illustrated and the definitions needed for the implementation of the method are given in these tables.

3.4 Workspace of n-RRRR and n-RRPR Manipulator Architectures

Once the workspace geometry of each chain is determined, the next step in the method is to identify all the points where the boundaries intersect. This is simply done by determining all the points of intersection each circle has with all the circles from the other chains.

Step 3 of the method is then to segment the circles into arcs at each of their points of intersection

Table 5: Conditions and radii of the workspace types resulting from Class 3 workspaces of Category A ($r_2 \leq 3r_1$).

Type	Condition	Radii	Figure
3	$L_4 < \left(\frac{r_2 - r_1}{2}\right)$	$r_{R1} = L_4 + r_1$ $r_{R2} = r_2 - L_4$ $r_{R3} = L_4 + r_3$	9
1	$\left(\frac{r_2 - r_1}{2}\right) \leq L_4 \leq r_1$	$r_{R3} = L_4 + r_3$	
2	$r_1 < L_4 < \left(\frac{r_2 + r_1}{2}\right)$	$r_{R0} = L_4 - r_1$ $r_{R3} = L_4 + r_3$	
2	$\left(\frac{r_2 + r_1}{2}\right) \leq L_4 < r_2$	$r_{R2} = r_2 - L_4$ $r_{R3} = L_4 + r_3$	Similar to 8(a)
1	$r_2 \leq L_4 \leq r_3$	$r_{R3} = L_4 + r_3$	Similar to 8(b)
2	$L_4 > r_3$	$r_{R0} = L_4 - r_3$ $r_{R3} = L_4 + r_3$	

Table 6: Conditions and radii of the workspace types resulting from Class 3 workspaces of Category B ($r_2 > 3r_1$).

Type	Condition	Radii	Figure
3	$L_4 \leq r_1$	$r_{R1} = L_4 + r_1$ $r_{R2} = r_2 - L_4$ $r_{R3} = L_4 + r_3$	9
4	$r_1 < L_4 < \left(\frac{r_2 - r_1}{2}\right)$	$r_{R0} = L_4 - r_1$ $r_{R1} = L_4 + r_1$ $r_{R2} = r_2 - L_4$ $r_{R3} = L_4 + r_3$	10(b)
2	$\left(\frac{r_2 - r_1}{2}\right) \leq L_4 < \left(\frac{r_2 + r_1}{2}\right)$	$r_{R0} = L_4 - r_1$ $r_{R3} = L_4 + r_3$	
2	$\left(\frac{r_2 + r_1}{2}\right) \leq L_4 < r_2$	$r_{R2} = r_2 - L_4$ $r_{R3} = L_4 + r_3$	Similar to 8(a)
1	$r_2 \leq L_4 \leq r_3$	$r_{R3} = L_4 + r_3$	Similar to 8(b)
2	$L_4 > r_3$	$r_{R0} = L_4 - r_3$ $r_{R3} = L_4 + r_3$	

with the other circles. A circle with n points of intersection is thus divided into n segments. After this step is complete, a list of segments can be drawn for each chain. Each segment is an arc that does not intersect with any other arc of any other chain.

Step 4 of the method is to determine which segments identified in Step 3 are a part of the boundaries of the workspace of the manipulator studied. To determine if a segment is part of the boundaries of the workspace of the manipulator in question, it is verified if the segment is inside the workspace of all the chains from which it does not originate. Since all segments have no intersection with any other segment, if one point of the segment is in the workspace of all other chains, then the entire segment is also in the workspace of all other chains. The mid point on the segment is used for this as it is easy to determine and is farthest to the ends of the segment. This

prevents potential errors due to the truncation of computational variables.

The fact that the workspace of each chain is defined by a number of concentric circles simplifies the process of testing whether or not a point is in its workspace. Note that the circles defined by r_{R0} and r_{R2} always define an inner limit to the workspace, i.e., a point in these circles is not in the workspace of the chain. Inversely, circles defined by r_{R1} and r_{R3} define an outer limit to the workspace. It is also important to note that the smaller circles take precedence in this matter. For example, if a point is in both circles defined by r_{R0} and r_{R1}, the circle defined by r_{R0} takes precedence and the point is not in the workspace. Following this logic, one way to determine if a point is in the workspace of a chain is to start with the smallest circle and work outward until the point is in the circle. Then if the first circle to include the point is defined by r_{R0} or r_{R2}, the point is not in the workspace of that chain. If the first circle to include the point is defined by r_{R1} or r_{R3}, the point is in the workspace. If the point is not in any circle, it is not in the workspace.

Once this test is done with all segments with all other chains, a list can be drawn of all the segments forming the boundaries of the workspace of the manipulator in question. At this point in the method, a geometric representation of the workspace of n-RRRR and n-RRPR manipulators is obtained.

Step 5 is used to obtain a scalar value of the area of the manipulator's workspace.The Gauss Divergence Theorem [6] is used to obtain the contribution of each segment that are all added to obtain the area of the workspace [10].

4 EXAMPLE WORKSPACE

To demonstrate the versatility of the method presented, an example of the workspace of a manipulator is presented in this section. The manipulator in question is a manipulator with four chains in total, two of them being of RRRR architecture and the other two of RRPR architecture. Figure 11(a) illustrates this manipulator and Table 7 shows the dimensions of each chain in this manipulator as well as the position of the base of each chain. Figure 11(b) shows the resulting workspace which has an area of 10.57.

Table 7: Dimensions of the example manipulator.

	Kinematic chain			
	1	2	3	4
Type	RRRR	RRRR	RRPR	RRPR
L_1 or L_1^{min}	2.01	1.80	0.20	0.50
L_2 or L_1^{max}	1.22	1.29	2.41	1.60
L_3	0.41	0.41	0.41	0.41
L_4	1.12	1.51	0.88	1.37
(X_3,Y_3)	(0.0 , 1.35)	(3.3 , 1.15)	(2.3 , 0.0)	(0.0 , 0.0)

5 CONCLUSIONS

The geometric method presented to determine the geometry of the dexterous workspace for kinematically redundant n-RRRR and n-RRPR planar manipulators is easy to implement. Based on the architectural parameters, the class determining the number of concentric circles of the workspace of the non-redundant chain is identified using Table 1 or Table 2. The associated radii are obtained using Eq. (1) or Eq. (2). The relationship between the redundant link length L_4 and the radii

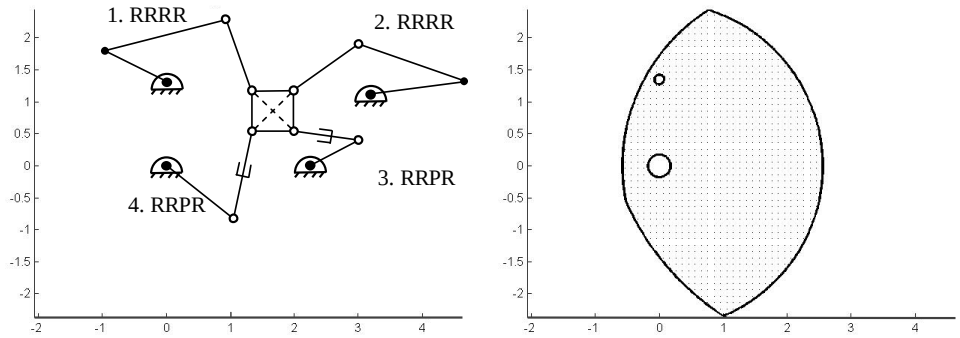

Figure 11: Example workspace of a planar parallel manipulator with a revolute redundant actuator.

of the classes dictates the type of workspace as seen in Tables 3-6. The method to determine the boundaries of the intersection of all the kinematic chains is simple since it only involves finding the intersection of circles.

The dexterous workspace of manipulators is an important criterion for their design. The implementation of this method is therefore a useful tool in the design of kinematically redundant planar parallel manipulators.

REFERENCES

[1] Gosselin, C., and Angeles, J., The optimum kinematic design of a planar three-degree-of-freedom parallel manipulator, ASME Journal of Mechanisms, Transmissions and Automation in Design, **110**(1):35–41, 1988.

[2] Williams II, R. L., and Reinholtz, C. F., Closed-form workspace determination and optimization for parallel robot mechanisms, In ASME Design Technology Conferences 20th Biennial Mechanisms Conf.:341–351, 1988.

[3] Kumar, V., Characterization of workspaces of parallel manipulators, ASME Journal of Mechanical Design, **114**(3):368–375, 1992.

[4] Zhaohui, L., and Zhonghe, Y., Determination of dexterous workspace of planar 3-dof parallel manipulator by auxiliary linkages, Chinese Journal of Mechanical Engineering (English edition), **17**(Suppl.):76–78, 2004.

[5] Merlet, J.-P., Gosselin, C., and Mouly, N., Workspace of planar parallel manipulators, Mechanism and Machine Theory, **33**(1-2):7–20, 1998.

[6] Buck, R. C., Advanced Calculus, International series in pure and applied mathematics, McGraw-Hill Book Company., 1965.

[7] Gosselin, C., Determination of the workspace of 6-dof parallel manipulators, ASME Journal of Mechanical Design, **112**(3):331–336, 1990.

[8] Ebrahimi, I., Carretero, J. A., and Boudreau, R., A family of kinematically redundant planar parallel manipulators, ASME Journal of Mechanical Design, **130**(6):062306–1– 062306–8, 2008.

[9] Gallant, A., Boudreau, R., and Gallant, M., Dexterous workspace of a 3-PRRR kinematically redundant planar parallel manipulator, Transactions of the Canadian Society for Mechanical Engineering, **33**(4):645–654, 2009.

[10] Gallant, A., Boudreau, R., and Gallant, M., Dexterous workspace of a n-PRRR planar parallel manipulators, Proceedings of the ASME 2010 IDETC, 2010.